Infrastructure and Environment Scotland 3rd Postgraduate Conference
9th December 2015
Heriot-Watt University, Edinburgh

An investigation of the accuracy of the partition of unity method for time dependent heat transfer problems

M. Iqbal[1,*], H. Gimperlein[2,3], M. S. Mohamed[1], O. Laghrouche[1]
[1]Institute for Infrastructure and Environment, Heriot Watt University
[2]Maxwell Institute for Mathematical Sciences and Department of Mathematics, Heriot Watt University
[3]Institute for Mathematics, University of Paderborn, Warburger Str. 100, 33098 Paderborn, Germany
[*](Email: mi130@hw.ac.uk)

ABSTRACT

This paper investigates the accuracy of the partition of unity method (PUM) for the solution of time dependent heat transfer problems. We propose a mathematically rigorous, computable error estimate and test the accuracy of PUM against this error estimate. It is shown that the proposed error estimate provides reliable and practically useful upper bounds for the numerical errors, independent of the heuristically chosen enrichment functions. We considered two model problems to test the method. First we considered a problem for which we know the exact mathematical solution. For the second case a problem is considered for which the exact solution is not known. We use different number of time steps to capture the results, and it is confirmed that at every time step the actual error in the solution is bounded by the error estimates.

1. INTRODUCTION

In recent years various generalized and meshless numerical methods have been introduced to solve complex engineering problems with ease and suffcient accuracy. One of the important subclass of these methods is the Partition of Unity Method PUM. This method was introduced by Melenk and Babuska [1], who developed the mathematical background of this method. They showed how the partition of unity finite element method can be used to employ the structure of the differential equation under consideration to construct effective and robust methods.

PUM used coarse meshes and incorporates special functions into the finite element space to approximate the solution. These special functions are called enrichment functions and are chosen based on an approximate analytical solution of the problem. To a great extent the effectiveness of the PUM depends on the proper selection of enrichment functions. Strouboulis *et al.* [2] showed that the choice of enrichment function affects the solution of the problem. The fact that PUM uses coarse meshes to approximate the finite element solution of complex problems, it is necessary to address the accuracy and reliability of this method.

PUM has found applications in wide variety of applications. This method is effectively used to solve engineering problems both in solid and fluid mechanics. Munts *et al.* [5] investigated the effectiveness of PUM for convection-diffusion problems. O'Hara *et al.* [3] used it for transient analysis of sharp thermal gradients. They used global-local enrichment functions to problems of transient heat transfer involving localized features. Laghrouche and Mohamed [4] used it for solving the Helmholtz equation in two dimensions. They constructed oscillatory shape functions as the product of polynomial shape functions and either Bessel functions or planer waves. In their work they dealt with the diffraction of an incident plane wave by a rigid circular cylinder. Duarte and Kim [6] used PUM for accurately modeling a crack using enrichment functions from the asymptotic expansion of the elasticity in the neighborhood of the crack. Mohamed *et al.* [7] used PUM for the solution of time dependent diffusion problems. They used multiple enrichment function to obtain the results. In their work they compared the results of both finite element method and PUM and concluded that in general the PUM shows higher accuracy than the conventional FEM for a fixed number of degrees of freedom. They showed that PUM requires less computational resources for the time-dependent diffusion problems than the standard FEM. A full description of previous work can be found in their work.

In our present work we define mathematically rigorous, computable error estimates. We use PUM to solve time-dependent diffusion problem and compare the actual errors in the solution the error estimates. For an acceptable numerical solution, the actual errors in the solution should be less than the error estimates. We define the governing PDE for transient diffusion problem with appropriate initial and boundary conditions and its transformation to weak form in the next section. In

Section 3, we define the error estimates followed by results of numerical analyses in Section 4. Some concluding remarks are presented in Section 5.

2. PROBLEM FORMULATION AND NUMERICAL APPROXIMATION

Given an open domain $\Omega \subset \mathbb{R}^2$ with boundary Γ and given time interval]0,T], we consider the following transient diffusion equation

$$\frac{\partial u}{\partial t} - \lambda \Delta u = f(t, \boldsymbol{x}), \quad (t, \boldsymbol{x}) \in]0, T] \, x \, \Omega \tag{1}$$

Where $\boldsymbol{x} = (x, y)^T$ are the spatial coordinates, u is the temperature, t is the time variable, $\lambda > 0$ is the diffusion coefficient and the right hand side $f(t, \boldsymbol{x})$ represents the effect of internal sources/sinks. We consider an initial condition

$$u(t = 0, \boldsymbol{x}) = u_0(\boldsymbol{x}), \quad (\boldsymbol{x} \in \Omega) \tag{2}$$

where $u_0(\boldsymbol{x})$ is a prescribed initial field. We impose Robin type boundary condition

$$\frac{\partial u}{\partial \boldsymbol{n}} + hu = g(t, \boldsymbol{x}), \quad (t, \boldsymbol{x}) \in]0, T] \, x \, \Gamma \tag{3}$$

here $\boldsymbol{n}$ denotes the outward normal on the boundary Γ, $h \geq 0$ is the convection heat transfer coefficient and g represents a given boundary function.

To solve equation (1)-(3) numerically, we divide the time interval into N_t subintervals $[t_n, t_{n+1}]$ with duration $\Delta t = t_{n+1} - t_n$ for $n = 0, 1, 2, \ldots N_t$. We discretize equation (1) in time using an implicit scheme.

$$\frac{u^{n+1} - u^n}{\delta t} - \lambda \Delta u^{n+1} = f(t_{n+1}, \boldsymbol{x}) \tag{4}$$

rearranging gives

$$-\Delta u^{n+1} + k u^{n+1} = F \tag{5}$$

where

$$F = k(\delta f(t_{n+1}, \boldsymbol{x}) + u^n), \quad k = \frac{1}{\lambda \delta t}$$

To solve equation (5) with the finite element method we first multiply the equation with a smooth test function, W, and then integrate over Ω

$$-\int_\Omega W \, \Delta u^{n+1} d\Omega + \int_\Omega W \, k u^{n+1} d\Omega = \int_\Omega W \, F d\Omega \tag{6}$$

Now suppose we have a function, S, such that

$$S = W \nabla u^{n+1} = \begin{pmatrix} W \dfrac{\partial u^{n+1}}{\partial x} \\ W \dfrac{\partial u^{n+1}}{\partial y} \end{pmatrix} \tag{7}$$

Taking divergence of the function S and applying the divergence theorem, we get

$$\int_\Omega (\nabla W . \nabla u^{n+1} + \mathrm{W} k u^{n+1}) d\Omega - \int_\Gamma W \nabla u^{n+1} . n \, d\Gamma = \int_\Omega W F \, d\Omega \tag{8}$$

Substituting the boundary conditions and rearranging, we get

$$\int_\Omega (\nabla W . \nabla u^{n+1} + W k u^{n+1}) d\Omega + \int_\Gamma W (k u^{n+1} - g) \, d\Gamma = \int_\Omega W F \, d\Omega \tag{9}$$

Our aim is to find an approximate solution of the weak form (9) using PUM. To do so, the temperature u over each element is approximated as

$$\mathrm{u} = \sum_{j=1}^{M} \sum_{\mathrm{q}=1}^{Q} A_j^q \, N_j(\boldsymbol{x}) \, G_q(\boldsymbol{x}) \tag{10}$$

Here $A_j^q \in \mathbb{R}$, and N_j are the piecewise polynomial shape functions. As in [7], we use the following global enrichment functions

$$G_q(\boldsymbol{x}) = \frac{e^{-\left(\frac{R_0}{C}\right)^q} - e^{-\left(\frac{R_c}{C}\right)^q}}{1 - e^{-\left(\frac{R_c}{C}\right)^q}}, \quad q = 1, 2, 3, \ldots . Q \tag{11}$$

with $R_0 := |\boldsymbol{x} - \boldsymbol{x_c}|$ being the distance from the function control point $\boldsymbol{x_c}$= (1,1) to the point $\boldsymbol{x}$. The constants $R_c = \sqrt{\frac{14}{1.195}}$ and $C = \sqrt{\frac{1}{1.195}}$ control the shape of the exponential function, G_q. Alturi and Zhu [8] also used an enrichment function similar to (12) with $q = 2$ as a weight function in the context of meshless methods for solving the linear Poisson equation. Similar functions are used when $q = 1$ in [5, 9] and $q = 2$ in [3, 10].

For simplicity we write the product of the enrichment function G_q with the polynomial shape function N_j as

$$P_{(j-1)q+Q} = N_j G_q \tag{12}$$

The derivatives of the new shape function are given as

$$\frac{\partial P_{(j-1)q+Q}}{\partial x} = G_q \frac{\partial N_j}{\partial x} - N_j(x - x_c)\frac{q}{C^q}\frac{e^{-\left(\frac{R_0}{C}\right)^q}}{1 - e^{-\left(\frac{R_c}{C}\right)^q}} R_0^{(q-2)}$$

and

$$\frac{\partial P_{(j-1)q+Q}}{\partial y} = G_q \frac{\partial N_j}{\partial y} - N_j(y - y_c)\frac{q}{C^q}\frac{e^{-(\frac{R_0}{C})^q}}{1 - e^{-(\frac{R_c}{C})^q}} R_0^{(q-2)}$$

The second derivatives of the new shape function are given as

$$\frac{\partial^2 P_{(j-1)q+Q}}{\partial x^2} = [-2\frac{\partial N_j}{\partial x}(x - x_c)\frac{q}{C^q}\frac{e^{-\left(\frac{R_0}{C}\right)^q}}{1 - e^{-\left(\frac{R_c}{C}\right)^q}} R_0^{(q-2)}$$
$$+N_j \frac{q}{C^q}\frac{e^{-\left(\frac{R_0}{C}\right)^q}}{1 - e^{-\left(\frac{R_c}{C}\right)^q}}(1 - \frac{q}{C^q}R_0^{(q-2)}(x - x_c)^2$$
$$+\frac{q-2}{R_0^2}(x - x_c)^2]$$

and

$$\frac{\partial^2 P_{(j-1)q+Q}}{\partial y^2} = [-2\frac{\partial N_j}{\partial y}(y - y_c)\frac{q}{C^q}\frac{e^{-\left(\frac{R_0}{C}\right)^q}}{1 - e^{-\left(\frac{R_c}{C}\right)^q}} R_0^{(q-2)}$$
$$+N_j \frac{q}{C^q}\frac{e^{-\left(\frac{R_0}{C}\right)^q}}{1 - e^{-\left(\frac{R_c}{C}\right)^q}}(1 - \frac{q}{C^q}R_0^{(q-2)}(y - y_c)^2$$
$$+\frac{q-2}{R_0^2}(y - y_c)^2]$$

3. DEFINITION OF ERROR ESTIMATES

In this section we define the error estimate for the method. We will then compare the results obtained by the PUM to the error estimate.

Let us define

$$u(\boldsymbol{x}, t) = \frac{t - t_n}{t_{n+1} - t_n} u^{n+1}(\boldsymbol{x}) + \frac{t_{n+1} - t}{t_{n+1} - t_n} u^n(\boldsymbol{x})$$

and

$$\hat{u}(\boldsymbol{x}, t) = u(\boldsymbol{x}, t_{n+1}), \dot{I}(\boldsymbol{x}, t) = f(\boldsymbol{x}, t_{n+1}), t \in [t_n, t_{n+1}]$$

Let u and U be the numerical and exact solution respectively of the equation (1), with

$$U(0, \boldsymbol{x}) = U_0(\boldsymbol{x}) \text{ and } U|_\Omega = 0$$

then

$$\int_\Omega |U(t_{(n+1)}, \boldsymbol{x}) - u(t_{(n+1)}, \boldsymbol{x})|^2 dx +$$
$$\lambda \int_{t_n}^{t_{n+1}} \int_\Omega |\nabla(U - u)|^2 d\boldsymbol{x}\, dt \le \eta_2^2 + \eta_4^2 + \eta_5^2 \qquad (13)$$

where

$$\eta_2^2 = \int_{t_n}^{t_{n+1}} ||f - \partial_t u - \Delta u||^2_{H^{-1}(\Omega)}$$
$$\le \int_{t_n}^{t_{n+1}} dt \int_\Delta (f - \partial_t u - \Delta u)^2 \, d\Omega$$
$$\cong \int_\Delta (f^{n+1} - \frac{u^{n+1} - u^n}{\delta t} - (\frac{\partial^2 u^{n+1}}{\partial x^2} + \frac{\partial^2 u^{n+1}}{\partial y^2}))^2 \frac{\delta t}{2} d\Omega$$
$$+ \int_\Delta (f^n - \frac{u^{n+1} - u^n}{\delta t} - (\frac{\partial^2 u^n}{\partial x^2} + \frac{\partial^2 u^n}{\partial y^2}))^2 \frac{\delta t}{2} d\Omega \qquad (14)$$

and

$$\eta_4^2 = \int_{t_n}^{t_{n+1}} ||\nabla(u - \hat{u}||^2_{L^2(\Omega)}$$
$$= \int_{t_n}^{t_{n+1}} \left(\frac{t_{n+1} - t}{t_{n+1} - t_n}\right)^2 dt \int_\Delta [(\frac{\partial u^{n+1}}{\partial x} - \frac{\partial u^n}{\partial x})^2 +$$
$$(\frac{\partial u^{n+1}}{\partial y} - \frac{\partial u^n}{\partial y})^2 \, d\Omega$$

Simplifying

$$= \frac{(t_{n+1} - t_n)}{3} \int_\Lambda [(\frac{\partial u^{n+1}}{\partial x} - \frac{\partial u^n}{\partial x})^2 +$$
$$(\frac{\partial u^{n+1}}{\partial x} - \frac{\partial u^n}{\partial x})^2] \, d\Omega \qquad (15)$$

$$\eta_5^2 = \sum_{\text{edges}} \int_{t_n}^{t_{n+1}} ||\frac{\partial \hat{u}}{\partial \boldsymbol{n}}||^2_{L^2(E)}$$
$$= \sum_{\text{edges}} \int_{t_n}^{t_{n+1}} ||\nabla u^{n+1}.\boldsymbol{n}||^2_{L^2(E)}$$
$$= \sum_{\text{edges}} \int_{t_n}^{t_{n+1}} dt \int_E [\left(\frac{\partial u^{n+1}}{\partial x}\, n1_x + \frac{\partial u^{n+1}}{\partial y}\, n1_y\right)_{E_1}$$
$$-\left(\frac{\partial u^n}{\partial x}\, n1_x \frac{\partial u^n}{\partial y}\, n1_y\right)_{E_2}] \, dE \qquad (16)$$

We will calculate the quantities defined in (13), and will then compare it with the error terms η_2^2 , η_4^2 and η_5^2. The left hand side of (13) quantifies the actual error in the numerical solution compared to the exact solution and the right hand side calculates the error indicator consisting of three terms η_2^2, η_4^2 and η_5^2. As defined by (13), the actual error in the solution should be less than or equal to the error indicator.

4. NUMERICAL ANALYSIS

Numerical results of the PUM for the proposed problem are presented here. We consider a square domain $\Omega = [0,2]\,\mathrm{x}\,[0,2]$ with heat diffusion coefficient $\lambda = 0.1\ kg\ m/C^0 s^2$ and convection heat transfer coefficient $h = 1\ kg/C^0 s^2$. We find numerical solution to heat transfer problem (1) - (3) with reaction term $f(t, \boldsymbol{x})$, the boundary function g.

For numerical analyses we choose square mesh with all integrals over Ω evaluated using Gauss-Legendre quadrature with 22 integration points.

To quantify the error for different model problems, we compute the relative error between the exact solution U and its PUM approximation u, defined as the square root of

$$\frac{\int_\Omega |U-u|^2 d\Omega + \lambda \int_{t_n}^{t_{n+1}} \int_\Omega |\nabla(U-u)|^2 d\Omega\, dt}{\int_\Omega |U|^2 d\Omega + \lambda \int_{t_n}^{t_{n+1}} \int_\Omega |\nabla U|^2 d\Omega\, dt} \qquad (17)$$

And the corresponding relative error indicator is defined as the square root of

$$\frac{\eta_2^2 + \eta_4^2 + \eta_5^2}{\int_\Omega |U|^2 d\Omega + \lambda \int_{t_n}^{t_{n+1}} \int_\Omega |\nabla U|^2 d\Omega\, dt} \qquad (18)$$

For the case where the exact solution U is not known, we use a reference FEM solution with very fine mesh instead.

4.1 Model Problem 1

For model problem 1 we select a problem for which the exact solution U is known. We solve the heat transfer problem (1) - (3) with reaction term $f(t, \boldsymbol{x})$, the boundary function g and the initial condition $u_0(\boldsymbol{x})$ chosen such that the exact solution is given by

$$U = x^{20} y^{20} (2-x)^{20} (2-y)^{20} (1 - e^{-\lambda t}) \qquad (19)$$

We use a coarse spatial mesh of 25 elements and vary the number of enrichment functions $Q = 2,3,,,6$. To quantify the error in the solution, we compute the actual error of the PUM solution and the error indicator as defined by (17) and (18) respectively. Figures 1(a)-1(c) show the comparison of these quantities for different number of enrichment functions Q and time steps δt at times $t = 0.1$ and $1\ s$. The number of enrichment functions Q are plotted on abscissa and the relative error, relative error indicator on the ordinate, both on logarithmic scale.

In all the cases the actual error of PUM solution is less than the error indicators. The error in solution decreases as we increase the number of enrichment functions. The error indicators also show similar decreasing pattern with the increase of enrichment functions and effectively capture the behaviour of numerical error in the solution.

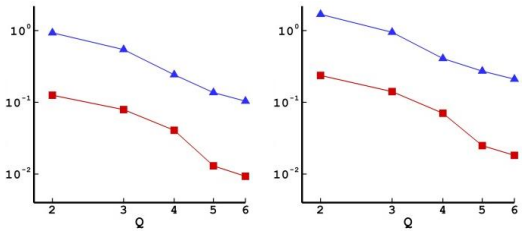

(a) (b)

Figure 1(a). Comparison of relative error (red line) and relative error estimate (blue line) at (a) 10th time step, (b) 100th time step for $\delta t = 0.0001\ s$

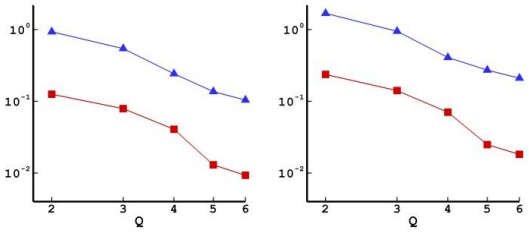

Figure 1(b). Comparison of relative error (red line) and relative error estimate (blue line) at (a) 10th time step, (b) 100th time step for $\delta t = 0.001\ s$

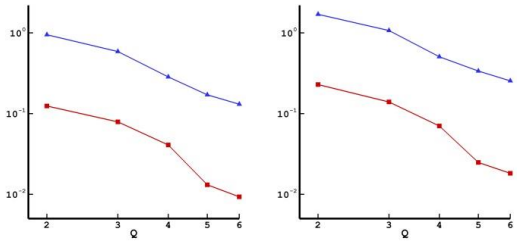

Figure 1(c). Comparison of relative error (red line) and relative error estimate (blue line) at (a) 10th time step, (b) 100th time step for $\delta t = 0.01\ s$

4.2 Model Problem 2

The model problem 2 considers a square domain with a heat source in the centre of domain as shown in figure 2. The source dissipates heat at two different rates. The centre part $x, y \in [0.8, 1.2]$ dissipates at constant rate $f = 200\ C^0/s$ and outside it f decreases linearly from $200\ C^0/s$ to 0 where either x, y is one of $\in [0.4, 1.6]$.

As the exact solution is not known in model problem 2, we only calculate the relative error indicator. As defined by (18), the exact solution U is replaced with a reference FEM solution on a very fine mesh of 12800 triangular elements. Both the PUM and FEM meshes are shown in figure 3.

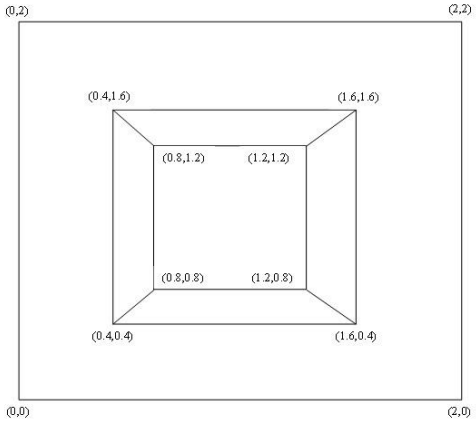

Figure 2. Domain configuration for model problem 2 with heat source in the centre.

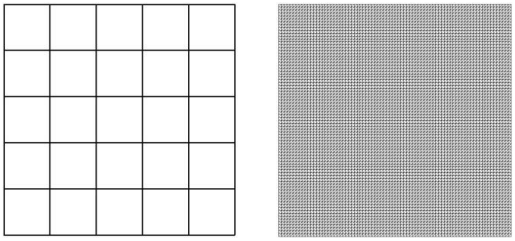

(a) PUM mesh (b) FEM mesh

Figure 3. Meshes used for the computations

Figures 4 (a) – (c) show the relative error indicator as a function of number of enrichment functions Q. Results are shown at $t = 0.01, 0.05$ and $0.1\ s$ using different values of time steps $\delta t = 0.001, 0.0001$ and $0.00001\ s$. The results show a decrease in the values of error indicator as we increase the number of enrichment functions. At early times results show similar trends for values of all values of δt (Figure 4(a)). At later time steps values decrease when we increase the number of Q from 2 to 4 but then increase when we further increase Q to 5 and 6. This can be clearly seen in Figure 4(c) specially for the smallest value of $\delta t = 0.00001\ s$. This is because the conditioning number of the system matrix deteriorates as we increase the number of enrichment functions. For $\delta t = 0.00001\ s$, the conditioning number increases from 1.5E+5 for $Q = 2$ to 2.0E+13 for $Q = 6$.

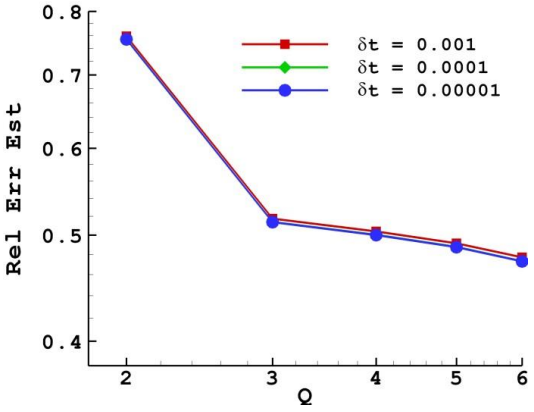

Figure 4(a). Relative error indicator at $t = 0.01\ s$

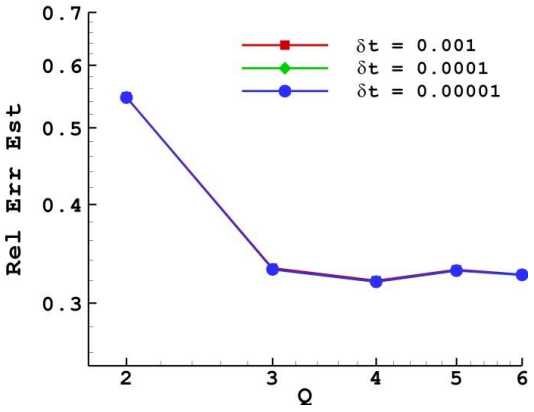

Figure 4(b). Relative error indicator at $t = 0.05\ s$

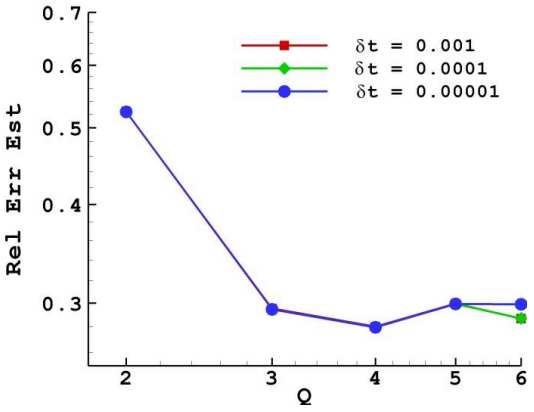

Figure 4(c). Relative error indicator at $t = 0.1\ s$

5. CONCLUSIONS

In this paper, we used the PUM to solve the time dependent heat diffusion equation. We calculated

the errors in the solution and its derivatives for the PUFEM. We defined an error estimate and compared the actual error in the method with the defined error estimate. We used different number of enrichment functions and showed their effect on the solution. Based on the analysis, we can draw the following conclusions:

- Results of the actual error are well below the defined error estimate and both show similar decrease with increasing number of enrichment functions.
- The proposed error estimates do not depend on the choice of enrichment function. These estimates are easy to implement and effectively reflect the behaviour of numerical error.
- The error indicators also reflect the errors incurred in the poorly conditioned systems.
- Increasing the number of enrichment functions produce better results but the enrichment functions can be increase only up to certain limit after which the system becomes ill-conditioned.

6. REFERENCES

[1] Melenk, J. M. & Babuška, I. (1996). The partition of unity finite element method: basic theory and applications. *Computer methods in applied mechanics and engineering*, *139*(1): 289-314.

[2] Strouboulis, T., Copps, K. & Babuska, I. (2000). The generalized finite element method: an example of its implementation and illustration of its performance. *International Journal for Numerical Methods in Engineering*, *47*(8): 1401-1417.

[3] O'Hara, P., Duarte, C. A. & Eason, T. (2011). Transient analysis of sharp thermal gradients using coarse finite element meshes. *Computer Methods in Applied Mechanics and Engineering*, *200*(5): 812-829.

[4] Laghrouche, O. & Mohamed, M. S. (2010). Locally enriched finite elements for the Helmholtz equation in two dimensions. *Computers & structures*, *88*(23): 1469-1473.

[5] Munts, E. A., Hulshoff, S. J. & Des Borst, R. (2003). The partition-of-unity method for linear diffusion and convection problems: accuracy, stabilization and multiscale interpretation. *International journal for numerical methods in fluids*, *43*(2): 199-213.

[6] Duarte, C. A. & Kim, D. J. (2008). Analysis and applications of a generalized finite element method with global–local enrichment functions. Computer Methods in Applied Mechanics and Engineering, 197(6): 487-504.

[7] S. Mohamed, M., Seaid, M., Trevelyan, J. & Laghrouche, O. (2013). A partition of unity FEM for time dependent diffusion problems using multiple enrichment functions. International Journal for Numerical Methods in Engineering, 93(3): 245-265.

[8] Atluri, S. N. & Zhu, T. (1998). A new meshless local Petrov-Galerkin (MLPG) approach in computational mechanics. Computational mechanics, 22(2): 117-127.

[9] Van der Meer, F. P., Al-Khoury, R. & Sluys, L. J. (2009). Time-dependent shape functions for modeling highly transient geothermal systems. International journal for numerical methods in engineering, 77(2): 240-260.

[10] O'Hara, P., Duarte, C. A. & Eason, T. (2009). Generalized finite element analysis of three-dimensional heat transfer problems exhibiting sharp thermal gradients. Computer Methods in Applied Mechanics and Engineering, 198(21): 1857-1871.